CRYSTAL GROWTH & DESIGN

ARTICLE

pubs.acs.org/crystal

# Chemical Kinetics of Gold Nanorod Growth in Aqueous CTAB Solutions

Craig Bullen,[†] Peter Zijlstra,[‡] Eric Bakker,[§,∥] Min Gu,[‡] and Colin Raston*[,†]

[†]Centre for Strategic Nanofabrication, School of Biomedical, Biomolecular and Chemical Sciences, University of Western Australia, Perth 6008, Australia

[‡]Centre for Micro-Photonics, Swinburne University of Technology, John St. Hawthorn, Australia

[§]Nanochemistry Research Institute, Curtin University, Western Australia, GPO Box U1987, Australia

Supporting Information

**ABSTRACT:** The chemical kinetics of the silver-mediated growth of gold nanorods prepared by the reduction of gold precursor in aqueous cetyltrimethylammonium bromide (CTAB) solution has been systematically studied using spectroscopic monitoring and electron microscopy. The rate of monomer depletion $-d[Au^{n+}]/dt$ has a linear dependence on both $[Au^{n+}]$ and seed nuclei concentration at 30 °C. Particle growth is significantly retarded by hexadecyltrimethylammonium bromide (CTAB) and KBr, with the order ca. −1 for $[Br^-]$. The rate of nanoparticle growth is dependent on the reducing ascorbate monoanion concentration and is consequently highly pH dependent around the $pK_a$[1] of ascorbic acid, while $AgNO_3$ retards the observed kinetics for both the growth of nanorods from ca. 2 nm seed nuclei and the overgrowth of Au nanorods.

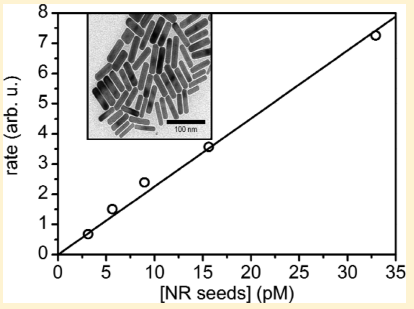


## INTRODUCTION

Nanoparticle size and shape are often kinetically determined through a balance of the rates of nucleation to facet-specific growth or aggregative coarsening processes.[1−3] The relative growth rates of the different nanocrystal facets can be regulated through nuclei structure, reaction conditions,[4] and facet-specific adsorbate effects, to promote anisotropic nanocrystal structure growth.[5,6] Understanding of the chemical factors affecting the growth kinetics of anisotropic nanocrystals is desirable from both synthetic and mechanistic standpoints. Herein, we present a systematic account of the chemical kinetics of nanoparticle growth for the facile silver-mediated synthesis of gold nanorods (AuNRs) in aqueous hexadecyltrimethylammonium bromide (CTAB) solution.[7−9] AuNRs are promising photothermal heat elements,[10−12] contrast agents for biological imaging,[13] and active media for optical data storage.[14,15]

The silver-mediated seeded method[16] for growth of single-crystal AuNRs from seeds in CTAB solutions has been modified by lowering the growth solution pH to 1−2[17] and through the use of cetyltriethylammonium bromide[18] and benzyldimethylammonium bromide[7] surfactants. These changes significantly retard particle growth rates as compared to reactions in CTAB solutions without modification and produce {100} and {110} enclosed AuNRs. On the other hand, Xiang reported that AuNRs nanorods can be overgrown with Au to produce octahedral particles enclosed entirely by {111} facets through the use of excess ascorbic acid (10:1 Au) during NR growth to promote kinetic preference of {111} facet growth. The bromide ions of CTAB are not passive in the system and have been shown previously to retard the growth rate of metal nanoparticles as a result of selective {111} facet oxidation.[6]

Jana and Murphy proposed that $Ag^+$ ions specifically block growth on the long sides of Au nanorods to promote anisotropic growth.[9] More recently, an Ag−CTAB complex has been used to produce AuNRs, with spectroscopic evidence supporting the argument that Ag atoms coat the nascent Au surfaces.[10] Moreover, Xiang et al. reported that AuNRs and nanoarrows produced by a silver-mediated method were found to have a Ag/Au ratio of between 0.03 and 0.08, which is comparable to the 7% Ag atoms estimated to be required for monolayer coverage of Ag on the particles.[3] Using an argument of surface blocking, silver ions would be expected to retard overall particle growth kinetics, although this has hitherto not been verified experimentally.

Previous studies of the kinetics of gold nanorod growth/overgrowth have employed techniques including: sulphide/thiol arrested growth,[19] atomic force microscope/electron microscopy of surface bound NPs,[20] single particle spectroscopy,[11] small angle X-ray scattering (SAXS),[12] and UV−visible absorption of NR in solutions. Becker has reported a linear 5 $nm^3/s$ volume increase rate for AuNRs overcoated with Au in 0.1 M CTAB. Despite the precise sizing information offered by techniques like SAXS, quenching/TEM, and single particle spectroscopy, no full systematic investigation of the chemical kinetics of the Ag-mediated AuNR system has been reported.

**Received:** December 9, 2010
**Revised:** June 14, 2011
**Published:** June 20, 2011

We have considered the kinetics of growth of gold nanorods from preformed seed nuclei in an aqueous solution containing CTAB, $AgNO_3$, $HAuCl_4$, and ascorbic acid, using UV−visible spectrophotometry to monitor their growth. An activation energy of 90 kJ/mol for this system was determined using this methodology.[21] While the use of bulk solution UV−vis spectroscopy may be relatively limited in its ability to provide direct physical measurements of individual particles, it has been employed for this study to broadly cover the chemical kinetics of the silver-mediated AuNR growth chemistry.

## EXPERIMENTAL SECTION

$HAuCl_4$ was obtained from AGR Matthey, Perth, Western Australia. $AgNO_3$ (99+%, Aldrich), ascorbic acid (99%, Ajax Fine Chemicals), CTAB (Tech., Lancaster), and $NaBH_4$ (Aldrich) were used as-received without further purification. Milli-Q water with resistance greater than 18 MΩ was used for the preparation of all solutions.

CTAB-stabilized Au nanoparticle seeds (∼2 nm in diameter) were prepared using the method of Nikoobakht et al.[7] Briefly, 0.6 mL of ice-cold 15 mM $NaBH_4$ was injected into a 10 mL of rapidly stirred solution of 0.25 mM $HauCl_4$ in 100 mM CTAB. The pale brown solution was left to age for at least 1 h prior before use, and a fresh seed solution was prepared for each self-consistent set of kinetic studies. Seeds prepared in this manner were determined to give comparable data between 1 and 5 h after preparation, providing a suitable window for the study.

The growth of seed particles involved adding seeds (between 2 and 100 μL typically) into an aqueous growth media comprised of CTAB (5−100 mM), $HAuCl_4$ (typically 0.25−0.5 mM), $AgNO_3$ (0.1 mM), and ascorbic acid (where [Asc]/[Au] = 1.5). For a representative growth experiment, 20 μL of seed solution was added to 5 mL of room temperature growth solution. A 50 mM concentration of CTAB solution was employed in the kinetics studies because of the significantly increased rate of reaction as compared with more typical AuNR synthesis conditions using 100 mM solutions, as this reduced the chance of seed aging effects influencing trends.

The silver-mediated method for nanorod growth is usually a seeded method, with 2−3 nm seed nuclei produced ex situ being grown in a growth solution. The method has proven to be reliable; however, the CTAB-stabilized seed solution used is temporally only stable for several hours, after which time seed particles aggregate. In this respect, studies were also made for the overgrowth of purified AuNRs as seeds, which are more temporally stable nuclei. Overgrowth presented below relates to two AuNRs prepared by the Ag-mediated method, differing only in the ratio of Ag:Au used in their synthesis (being 1:4 and 1:7, described in the Supporting Information).

## INSTRUMENTATION AND ANALYSIS

Nanoparticle growth was monitored by UV−visible spectroscopy using either a Shimadzu UV-1601 or Ocean Optics USB2000$^+$ spectrometer, and spectra were acquired every 1−30 s depending on the rate of reaction. Raw spectra were integrated between 400 and 1000 nm, and the area obtained was divided by the area of a spectrum acquired at the end of the growth reaction and plotted against time to produce normalized growth curves. The maximum gradient of the integrated absorbance−time graph has been employed as a means of comparing the rates of reaction under different conditions. Two methods were used to determine the maximum gradients/rates. For the growth of small seed particles, maximum rates were obtained from a fit of the data with the Boltzmann

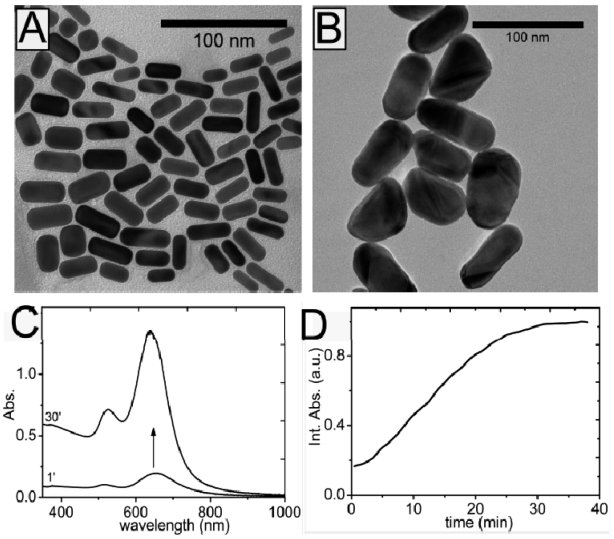


**Figure 1.** Electron micrographs of AuNR seeds (A) before and (B) after growth reaction. The corresponding UV−vis spectra before and after growth are shown in panel C, and in D, the kinetics curve of absorbance against time is presented, with sigmoidal Boltzmann curve fit (solid line). $T$ = 30 °C, [ascorbic acid] = 0.4 mM, [$HAuCl_4$] = 0.25 mM, and [CTAB] = 50 mM.

sigmoid having the form:

$$A_f = \frac{A_f - A_i}{1 + e^{x - x0/dx}} + A_i \qquad (1)$$

where $A_i$ = initial absorbance value, $A_f$ = final absorbance value, $x0$ = center, and $dx$ = time constant. In the following, the reciprocal of the time constant, $1/dx$, which is related to the maximum gradient of the sigmoidal curve, has been used as the rate of reaction.

To compare the growth rates for overgrowth of AuNR seeds, the change in absorbance at early times was found to be linear, and the initial gradient provides a convenient way to compare maximum growth rates for a comparable series of reactions at times when the seed geometry/faceting would not have changed too much. An assumption made in our analysis is that the yield of reaction is constant across a given reaction series, although in most cases the conversion of Au(III) monomer to Au(0) nanoparticles was found to be less than quantitative.

## RESULTS AND DISCUSSION

Growth data for a model reaction of preformed and purified AuNRs are presented in Figure 1. Transmission electron microscopy (TEM) micrographs of the initial AuNRs and of the particles after the growth reaction are shown in Figure 1A,B, respectively. The lengths and widths of >100 particles for the initial and final samples were measured, and particle volumes were determined assuming a cylindrical particle geometry. The mean particle width doubled from 13 ± 3 to 26 ± 6 nm, and the average length increased from 40 ± 11 to 63 ± 13 nm for these particular conditions, with the ratio of average end/side growth = 1.76. The TEM images also reveal more irregular shapes of the overgrown particles as compared with the AuNR seeds.

The ratio of initial and final mean volumes $V_f/V_i$ was determined to be 6.2 ± 0.9. In panels C and D, the optical changes in

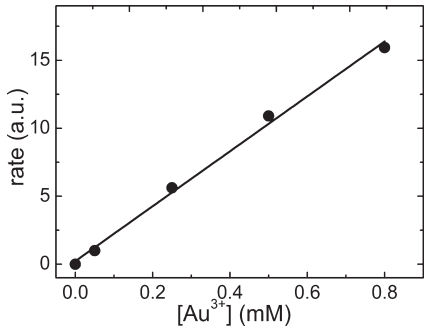


**Figure 2.** Gold nanorod growth rates as a function of added [$HAuCl_4$]. [CTAB] = 100 mM, [$AgNO_3$] = 0.12 mM, and [ascorbic acid] = 1.0 mM. Four microliters of CTAB-seed solution was used per mL of growth solution.

the system are presented, with the initial and final absorbance spectra shown in panel C. The increase in absorbance, taken as either the absorbance at the LSP peak maximum or the area under the absorbance curve between 400 and 1000 nm, was 6.0, within 5% of the TEM result. The increase in particle volume therefore correlates well for the growth of gold particles in this case, where there was not a large change in particle aspect ratio, and consequently, the LSP peak position only shifts slightly during particle growth (panel C).

In Figure 1D, the temporal evolution of the optical spectra for the Au nanorod overgrowth reaction is presented, with the characteristic sigmoidal Boltzmann growth curve obtained for the plot of the integrated areas against time. Previously, we have used $1/\tau_{1/e}$ of the sigmoid as an estimate of reaction rate, but herein, the maximum slope of the growth curve has been obtained from $1/dx$. For the representative growth curve for the overgrowth reaction shown in Figure 1, $dx$ is determined to be 6.3 ± 0.1 min, and accordingly, $1/dx$ is 0.15 $min^{-1}$ for the normalized curve. Using the known [$Au^{3+}$] = 0.25 mM and *assuming* a quantitative growth, the rate of decrease of monomer concentration is thus estimated to be 0.16 $\mu M\ s^{-1}$. In reality, the yield will not be quantitative;[22] however, by taking this value for maximum gradient and assuming cylindrical particles with an extinction coefficient of $3 \times 10^9\ M^{-1}\ cm^{-1}$, an average Au atom deposition rate of ca. 3 atoms per $nm^2/s$ is estimated, which is loosely consistent with the value for $dlength/dt$ of 0.14 nm/s reported by Gulati et al. for a similar AuNR growth and who modeled the evolving AuNR optical spectra using Gans' theory.[23]

The dependency of Au NR growth rate on the initial [$Au^{3+}$] present in the growth solution is presented in Figure 2. A reasonable linear relationship between [$Au^{3+}$] and particle growth rate was found for [$Au^{3+}$] < 1 mM, suggesting a first order dependence of the reaction on the initial [$HAuCl_4$]. The concentration window studied here covers the typical range of [$HAuCl_4$] employed for the preparation of AuNRs, although we do point out that Jana also prepared AuNRs using a 100 mM solution in a "gram scale" system, indicating that the ratio of reagents and not the absolute concentration is important for nanorods growth.[24] A plateau in the growth rate as a function of [$HAuCl_4$] plot is not apparent in Figure 2 for the concentration range that we have investigated, which is representative of most AuNR syntheses. The linear dependence is intuitively sensible if the rate of monomer deposition $-d[Au^{n+}]/dt$ is dependent on the amount of available monomer, with the depletion of Au

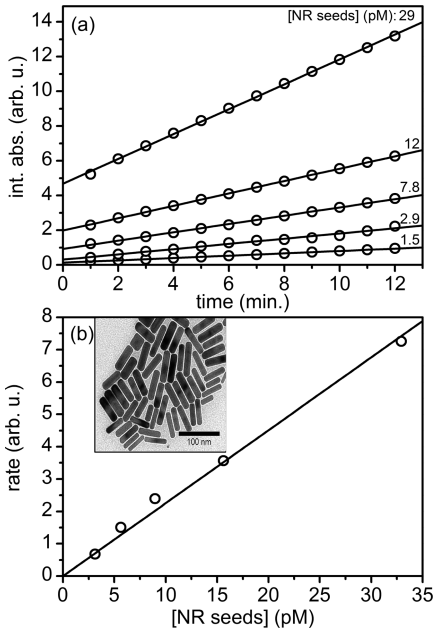


**Figure 3.** (a) Temporal dependence of the integrated absorbance for the growth 14 ± 4 nm by 52 ± 11 nm AuNR seeds injected into growth solutions containing [CTAB] = 30 mM, [$HAuCl_4$] = 0.25 mM, and [ascorbic acid] = 0.375 mM. (b) The growth rates for each curve in panel a plotted as a function of the concentration of nanorod seeds. The inset shows a TEM image of the nanorod seeds, and the scale bar indicates 100 nm. $T$ = 27 °C.

monomer accounting for the upper plateau in the sigmoidal curves (see Figure 1D).

The formation of Au(0) in this system requires an existing metal surface, which is known to catalyze the decomposition of ascorbic acid.[25] If the availability of reactive metal surface may be a limiting kinetic parameter in the depletion of monomer by gold particle growth, then the increase in rate in the first half of the growth curve can be accounted for by the increase in available surface during particle growth. It is reasonable that the rate of a surface deposition process could be related to the available surface area. To test this, overgrowth reactions of preformed and purified AuNRs with average dimensions of 13.7 ± 3 nm × 53 ± 10 nm were conducted, with [AuNR seed] systematically varied using a growth solution comprised of 30 mM CTAB, 0.25 mM $Au^{3+}$, and 0.375 mM ascorbic acid solution. Preformed nanoparticles were used in preference to the tiny CTAB-capped seeds whose physical dimensions are less well-defined and less stable, making an estimate of active surface area more difficult. The available surface area for the reactions was calculated from the number of added NR seeds, which was determined using an extinction coefficient of $4.8 \times 10^9\ M^{-1}\ cm^{-1}$.[9] To ensure that the change of surface area during the nanoparticle growth did not affect the maximum rates obtained, data from the first period of up to 12 min after seed addition were considered for maximum rate determination.

In Figure 3A, we present the temporal evolution of integrated absorbance for several reactions differing only by the amount of added NR seeds. In each case, a linear temporal absorbance change was observed in the first 12 min, with the gradient increasing with the amount of added seeds. These gradients, representing the maximum rate for each overgrowth reaction, are plotted in Figure 3B against the concentration of seed

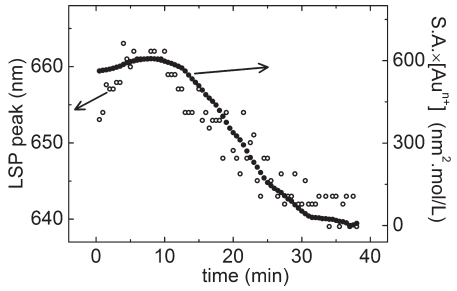


**Figure 4.** Temporal changes to LSP peak wavelength and $[Au^{+}] \times$ (total NR surface area) during the growth of AuNR seed nanoparticles. $T$ = 30 °C, [ascorbic acid] = 0.4 mM, $[HAuCl_4]$ = 0.25 mM, and [CTAB] = 50 mM.

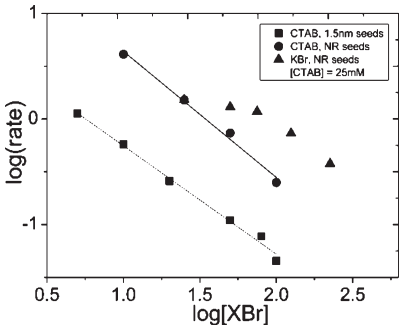


**Figure 5.** Gold nanoparticle grow rates as a function of [CTAB] for reactions seeded with ca. 1.5 nm CTAB stabilized seeds (●) or Au NR seeds (■). $[HAuCl_4]$ = 0.25 mM, $[AgNO_3]$ = 0.06 mM, and [ascorbic acid] = 0.375 mM. Closed triangles (▲) correspond to the rates of CTAB-seed growth, with [CTAB] = 25 mM and additional Br ions added in the form of KBr. Gradients of −1.2 were obtained for AuNR seeds and −1.0 for 1.5 nm seeds.

particles with a representative microscope image of the seed particles inset. The linear fit confirms the relationship between monomer consumption and the amount of NP surface area in the system.

Increasing the number of nanorods in solution produces to a proportional increase in the rate of monomer depletion. This correlation is interpreted to indicate that key rate-determining process involves attachment or desorption of some undetermined species on the surface of existing gold nanoparticles. It has been noted previously that the reduction of Au(III) to Au(0) by ascorbic acid in CTAB solution does not proceed on a time scale of hours to days, and here, we have indirectly found that Au ions reduction to metallic Au(0) is certainly enhanced by a high metal surface area.

The effect of dynamically changing particle surface area (SA) and monomer $[Au^{n+}]$ was explored further. On the basis of the data presented in Figure 1, monomer depletion and particle surface area increase should have opposing (increasing/decreasing respectively) effects on the nascent nanoparticle growth kinetics and could help account for the sigmoidal shape of the overgrowth curve.

In Figure 4, we present the temporal changes to the product of $[Au^{n+}]$ and total surface limiting conditions, and fast monomer deposition promotes nanoparticle surface area parameters plotted against the observed changes in nascent AuNR optical properties (LSP absorbance peak position). Surface areas of initial and final AuNR samples were determined using TEM data and assuming a cylindrical AuNR morphology. Intermediate particle dimensions during growth were inferred from the extent of reaction given by the sigmoid obtained from the absorbance spectra. The small red shift in the LSP peak occurs at early times when the overall growth rate is highest, but at longer reaction times, the depletion of monomer is the dominant kinetic factor and the rate decreases, with an associated 20 nm blue shift in the LSP observed (Figure 4).

A peak in kinetics for this model reaction was reached in the first 10 min, when $[HAuCl_4]$ was at a maximum, after which time the relative change in surface area becomes small as compared with the rapidly depleting Au monomer concentration. The high initial Au concentration and reaction-limiting surface may provide the kinetically controlled conditions required for preferential facet growth, while reduced rate at later times and a corresponding spectral blue shift indicate that conditions become less suitable for anisotropic growth. The changed morphology of the AuNRs at the end of the reaction may play a role here, too. The initial red shift could also arise from initial changes in the faceting of the AuNR seeds. Importantly, the use of ultrasmall seeds would lead to a much more significant initial change in available surface area and would extend the period before the monomer concentration becomes limiting. From a kinetics perspective, this could account for the observed limitation in the "standard" silver-mediated AuNR synthesis to ca. aspect ratio 5−6 in CTAB.[7]

We next consider the effect of the CTAB surfactant and bromide ions. In Figure 5, a plot of the dependence of the growth rates of both ultrasmall CTAB seed particles (filled circles) and AuNR seeds (filled squares) on [CTAB] is presented. In addition, for the AuNR seeds, the effect of varied [KBr] on the kinetics in 25 mM CTAB growth solution is presented (filled triangles). The strong and clear reciprocal relationship between rate and [CTAB] indicates that an effect of CTAB in AuNR formation is to dramatically retard Au nanorod growth. The order of reaction in [CTAB] was close to −1 for both ultrasmall and NR seed growth (−1 and −1.2, respectively).

Three processes associated with the CTAB in the system are the formation of [CTA−Au−Br] complexes, halide effects of the bromide counterion on nascent particles, and the formation of a surfactant bilayer stabilizing the nascent particles. All three would be expected to retard particle growth in some respect.

It has long been appreciated that CTAB associates strongly with both the NP surfaces (forming a bilayer) and the Au, Ag ions (forming CTA−M−Br complexes), while bromide ions are known to select against {111} faceting by a process of oxidative etching to promote the facet-specific AuNR growth seen.[6] To delineate the kinetic effects of the halide and surfactant, [KBr] was varied for a series of AuNR seed growth experiments. The effect of the initially added KBr was minimal, followed by the curve forming a linear region at higher KBr, again with gradient close to −1. The initial effect is sensible, since the NP growth occurs inside a rigid bilayer surfactant structure, where the bromide ions will be in relatively high local concentrations and a large proportion of the initially added KBr will stay in the bulk of solution. The gradient at higher [KBr], however, is close to the −1 seen for the two CTAB-only curves. On the basis of this analysis, we can conclude that the kinetic inhibition seen in this system as [CTAB] can be mostly attributed to the bromide ion.

In a recent study where CTAB was replaced by the related cetyltriethylammonium bromide (CTEAB), AuNR with aspect ratios up to 50 and the overall particle growth rate were reduced

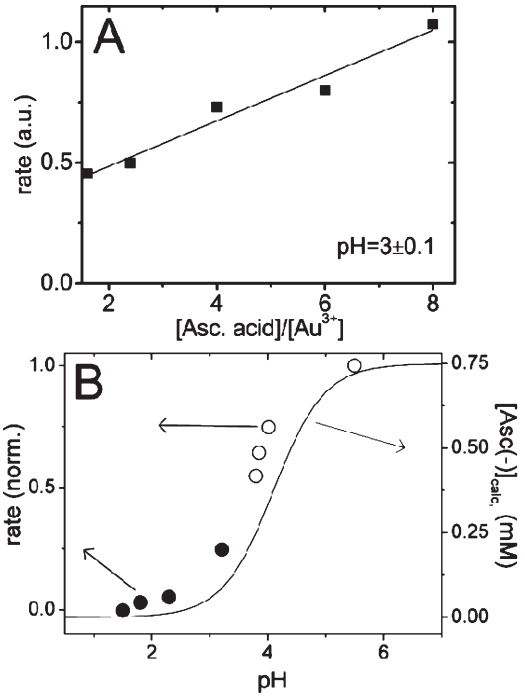


**Figure 6.** [Ascorbic acid] and pH dependence of AuNR growth rate in aqueous CTAB solution. (A and B) $T$ = 30 °C, [CTAB] = 100 mM, [Au] = 0.5 mM, [Ag] = 0.1 mM, and [ascorbic acid] = 0.75 mM, using 1.5 nm CTAB Au NPs. (B) Rate of AuNR seed growth as a function of pH. Open circles relate to 50 mM acetate-buffered solutions, while the closed circles correspond to unbuffered systems, respectively.

by 5-fold as compared with that observed for CTAB. This may be due to changed affinity/stability of the Au/$NR_4^+$ complex or perhaps the accessibility of the Au−CTAB to the surface, or alternatively, it reflects the role of the bilayer surfactant layer on the NP surface, providing more of a barrier for monomer deposition like increased viscosity. We do note, however, that viscosity measurements of CTAB solutions are not largely above those of water (100 mM CTAB viscosity 1.3 Cp). This all serves to highlight the importance of regulating kinetics in the formation of gold nanorods, with ammonium bromides being important for a number of reasons in this system. We do note, however, that in the related polyol synthesis of single crystal AuNRs in the presence of PVP, bromide ions were analogously able to regulate particle shape, with the selective {111} facet oxidation mechanism proposed.

The role of ascorbic acid in the AuNR growth system as reductant is to ultimately reduce the Au(III) to Au(0). This is a two-step process with a minimum [ascorbic acid]/[Au(III)] = 1.5 for good yields of Au(0). The first equivalent of the 2-electron donating ascorbic acid reduces Au(III) to Au(I) prior to seed addition. In our hands, the time after addition of ascorbic acid and the subsequent nucleation event (strong base or seed addition) could be at least 2 h without significant change in reaction outcome. We also note here that the initial loss of orange color upon addition of ascorbic acid occurs less than a few seconds and is not dependent on the [CTAB].

In Figure 6A, the effect of [ascorbic acid] on the growth rate of 1.5 nm seed particles is presented. A linear increase in reaction rate can be seen with increased [ascorbic acid], although this was only a doubling in rate with ca. 6-fold increase in [ascorbic acid]

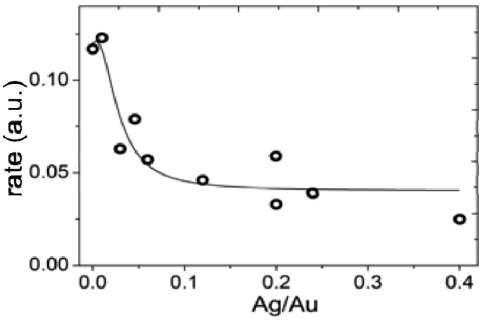


**Figure 7.** Rate of AuNR seed overgrowth with different added [$AgNO_3$]. [$HAuCl_4$] = 0.25 mM, [CTAB] = 50 mM, [ascorbic acid] = 0.375 mM, and $T$ = 30 °C.

at pH 3 ± 0.1. The p$K_a$ of ascorbic acid is 4.1, and it is the ascorbate monoanion that has been previously identified as the active reductant in the system. Ascorbic acid and a number of associated ions can exist in aqueous solution. Slowing the rate of reaction by lowering pH and keeping the [ascorbate]/[Au] below 6.2 has been found to be useful to slow growth and produce good yields of single crystalline AuNRs.[26]

The availability of ascorbate monoanion can be regulated by varying the pH around the p$K_a^1$ of 4.1. Figure 6B shows the rate of AuNR seed growth in acidic solutions, with the pH varied between 1.5 and 5.5. Because of the generation of $H^+$ during reduction of Au(I) to Au(0), it was necessary to buffer solutions with pH above 3.5 using 0.05 M acetate buffers. Interestingly, the buffers did not seem to affect the kinetics significantly. Comparison of the reaction rate data to the calculated pH dependence of [ascorbate] for 0.75 mM ascorbic acid in water indicates clear kinetics-based evidence that the ascorbate monoanion is the primary reductant involved in the growth of Au nanorods.[27]

The remaining parameter is the effect of silver-ion concentration on the kinetics of Au NR growth (Figure 7). Silver posed a significant challenge using our simple optical method since the large spectral changes seen with varied [$AgNO_3$] in the seeded growth method introduces significant uncertainty in interpreting relative growth rates. This was overcome by using preformed and thoroughly purified AuNRs as seed particles.

In Figure 7, it can be seen that $AgNO_3$ has a significant effect on the growth of Au nanorods. In particular are solutions with Ag/Au of 0.05−0.2, which represent the need to control the optical properties of AuNRs prepared by the silver-mediated method. These data reveal a small decrease in growth rate in this range of between 25 and 50% with increasing [$AgNO_3$]. Silver−CTAB complexes have recently been shown to be likely species in the AuNR system, while a popular mechanism for Ag-mediated AuNR formation is the preferential facet under potential deposition (UPD) of Ag ions on the nascent particles.[17,28] The present kinetics data could support a mechanism involving Ag atoms/complexes retarding the growth of side facets to promote AuNR growth.

In conclusion, a systematic investigation of the kinetics of silver-mediated AuNR growth has revealed the reaction to be first order in [$Au^{n+}$], first order in nanoparticle surface area, and surface limited. Depletion of monomer causes a peak in anisotropic growth, and on the basis of kinetics, the late blue shift seen in the system can be appreciated. The kinetics are highly pH dependent around the p$K_a^1$ (4.1) of ascorbic acid. The reaction rate is inversely related to [CTAB], mainly due to the selective


dx.doi.org/10.1021/cg101636r |*Cryst. Growth Des.* 2011, 11, 3375–3380

oxidative etching effect of the bromide counterion on Au {111}. The particle shape control provided by silver ions is associated with a reduction in particle growth rate. For the first time, the chemical kinetics of the silver-mediated AuNR system have been systematically investigated and have provided insights into anisotropic particle formation in this system.

## ■ ASSOCIATED CONTENT

**Supporting Information.** Detailed experimental details, spectra obtained, and growth curves. This material is available free of charge via the Internet at http://pubs.acs.org.

## ■ AUTHOR INFORMATION

### Corresponding Author

*E-mail: colin.raston@uwa.edu.au.

### Present Addresses

[||]University of Geneva, Quai E.-Ansermet 30, 1211 Geneva, Switzerland.

## ■ ACKNOWLEDGMENT

We are thankful for the support of the Australian Research Council, the West Australian Nanochemistry Research Institute, and the Centre for Microscopy and Microanalysis at the University of Western Australia, which is supported by University, State, and Federal Government funding.

## ■ REFERENCES

(1) Peng, X.; Wickham, J.; Alivisatos, A. P. *J. Am. Chem. Soc.* **1998**, *120*, 5343.
(2) Hu, Z.; Oskam, G.; Penn, R. L.; Pesika, N.; Searson, P. C. *J. Phys. Chem. B* **2003**, *107*, 3124.
(3) Xiang, Y. J.; Wu, X. C.; Liu, D. F.; Feng, L. L.; Zhang, K.; Chu, W. G.; Zhou, W. Y.; Xie, S. S. *J. Phys. Chem. C* **2008**, *112*, 3203.
(4) Berhault, G.; Bausach, M.; Bisson, L.; Becerra, L.; Thomazeau, C.; Uzio, D. *J. Phys. Chem. C* **2007**, *111*, 5915.
(5) Grzelczak, M.; Sanchez-Iglesias, A.; Rodrıguez-Gonzalez, B.; Alvarez-Puebla, R.; Perez-Juste, J.; Liz-Marzan, L. M. *Adv. Funct. Mater.* **2008**, *18*, 3780.
(6) Xiong, Y.; Cai, H.; Wiley, B. J.; Wang, J.; Kim, M. J.; Xia, Y. *J. Am. Chem. Soc.* **2007**, *129*, 3665.
(7) Nikoobakht, B.; El-Sayed, M. A. *Chem. Mater.* **2003**, *15*, 1957.
(8) Liz-Marzan, L. M.; Perez-Juste, J.; Mulvaney, P. *Abstr. Am. Chem. Soc.* **2005**, *229*, U731.
(9) Orendorff, C. J.; Murphy, C. J. *J. Phys. Chem. B* **2006**, *110*, 3990.
(10) Hubert, F.; Testard, F.; Spalla, O. *Langmuir* **2008**, *24*, 9219.
(11) Becker, J.; Schubert, O.; Sonnichsen, C. *Nano Lett.* **2007**, *7*, 1664.
(12) Morita, T.; Tanaka, E.; Inagaki, Y.; Hotta, H.; Shingai, R.; Hatakeyama, Y.; Nishikawa, K.; Murai, H.; Nakano, H.; Hino, K. *J. Phys. Chem. C* **2010**, *114*, 3804.
(13) Agarwal, A.; Huang, S. W.; O'Donnell, M.; Day, K. C.; Day, M.; Kotov, N.; Ashkenazi, S. *J. Appl. Phys.* **2007**, *102*.
(14) Zijlstra, P.; Chon, J. W. M.; Gu, M. *Nature* **2009**, *459*, 410.
(15) Chon, J. W. M.; Bullen, C.; Zijlstra, P.; Gu, M. *Adv. Funct. Mater.* **2007**, *17*, 875.
(16) Nikoobakht, B.; El-Sayed, M. A. *Chem. Mater.* **2003**, *15*, 1957.
(17) Liu, M.; Guyot-Sionnest, P. *J. Phys. Chem. B* **2005**, *109*, 22192.
(18) Kou, X.; Zhang, S.; Tsung, C.-K.; Yeung, M. H.; Shi, Q.; Stucky, G. D.; Sun, L.; Wang, J.; Yan, C. *J. Phys. Chem. B* **2006**, *110*, 16377.
(19) Zweifel, D. A.; Wei, A. *Chem. Mater.* **2005**, *17*, 4256.
(20) Liao, H.; Hafner, J. H. *J. Phys. Chem. B* **2004**, *108*, 19276.
(21) Zijlstra, P.; Bullen, C.; Chon, J. W. M.; Gu, M. *J. Phys. Chem. B* **2006**, *110*, 19315.
(22) Orendorff, C. J.; Murphy, C. J. *J. Phys. Chem. B* **2006**, *110*, 3990.
(23) Gulati, A.; Liao, H.; Hafner, J. H. *J. Phys. Chem. B* **2006**, *110*, 22323.
(24) Jana, N. R. *Small* **2005**, *1*, 875.
(25) Novo, C.; Funston, A. M.; Mulvaney, P. *Nature Nanotechnol.* **2008**, *3*, 598.
(26) Miranda, O. R.; Dollahon, N. R.; Ahmadi, T. S. *Cryst. Growth Des.* **2006**, *6*, 2747.
(27) Huang, C.-C.; Yang, Z.; Chang, H.-T. *Langmuir* **2004**, *20*, 6089.
(28) Grzelczak, M.; Perez-Juste, J.; Mulvaney, P.; Liz-Marzan, L. M. *Chem. Soc. Rev.* **2008**, *37*, 1783.